

# INFLUENCE OF LARGE STRAIN RHEOLOGY ON THE ADHESIVE PERFORMANCES OF PSA

Matteo Ciccotti<sup>1,\*</sup>, Richard Villey<sup>1,2</sup>, Costantino Creton<sup>1</sup>, Pierre-Philippe Cortet<sup>2</sup>, David J. Yarusso<sup>3</sup>

<sup>1</sup>Laboratoire SIMM (ESPCI Paristech, UPMC, CNRS), Paris, France

<sup>2</sup>Laboratoire FAST (Univ Paris Sud, CNRS), Orsay, France

<sup>3</sup>3M Center, 3M Company, St. Paul, MN, USA

\*e-mail: matteo.ciccotti@espci.fr

## Introduction

During the peeling of a Pressure Sensitive Adhesive (PSA), the adherence energy  $\Gamma$  is several orders of magnitude above the thermodynamic Dupré energy  $w$  between the adhesive and the underlying substrate, demonstrating the dominant role of energy dissipation. Moreover,  $\Gamma$  has a strong dependency on the peeling velocity  $V$ , and the characteristic  $\Gamma$  vs.  $V$  curves obey to a time-temperature superposition principle with a similar scaling to that of the linear rheology of adhesives. This has suggested for a long time that small strain viscoelasticity can be used to predict  $\Gamma$ , leading to two main modeling strategies.

The first approach<sup>1-3</sup> relates back to the sixties and uses the strong lateral confinement of the adhesive in a thin layer to treat it as a (visco)elastic foundation, constituted by a parallel array of springs (and dashpots) linking the flexible tape backing to the underlying substrate. Energy dissipation occurs in the whole thickness of the adhesive and it affects a stress concentration region beyond the peeling front (inside the bonded joint). The link with rheology is made through the time scale associated to the strain of this region caused by the propagation of the peeling front at velocity  $V$ . The characteristic peak of dissipation, which is responsible for the stick-slip instability, happens at the peeling velocity corresponding to the crossing of the glass transition.

In the second approach<sup>4-6</sup>, dissipation is obtained by a viscoelastic perturbation of the inverse square root stress singularity of LEFM (Linear Elasticity Fracture Mechanics). Energy dissipation happens in a region neighboring the crack front where the local strain rate (associated with the crack front propagation velocity  $V$ ) corresponds to the relaxation time of the adhesive. In these models, the peak in  $\Gamma(V)$  is obtained when the size of this dissipative region becomes comparable with the adhesive thickness.

In this second approach, the adherence energy  $\Gamma(V)$  is interpreted as an interfacial fracture energy amplified by viscoelasticity and should therefore be independent of the geometry and loading conditions of the adhesive joint. On the contrary,  $\Gamma(V)$  in the first approach is associated to the deformation of the whole adhesive joint, where the crack tip singularity plays a minor role. For this reason, the measured adherence energy  $\Gamma$  should be more properly interpreted as a work of debonding, which is rather an apparent fracture energy since it is not a fundamental property of the interface between the adhesive and the substrate.

Phenomenologically, the  $\Gamma(V)$  curves of soft confined adhesives were shown to be dependent on the adhesive

thickness  $a$  and on the peeling angle  $\theta$ , which tends to be in favor of the first approach<sup>7</sup>. However, data in the literature are related to very different types of adhesives, especially concerning their liquid/solid behavior. When considering soft solids only (such as most commercial PSA), which typically debond in an interfacial failure mode, this first approach, especially Kaelble's model<sup>1</sup>, seems to describe quite well the peeling experiments. This essentially linear elastic model (where the storage modulus might possibly be modulated by viscoelasticity) has however an unclear mechanical foundation. Even in a purely Hookean material, it would lead to a large and geometry dependent energy dissipation. This is in contradiction with the energy analysis of Griffith, which can also be applied to soft elastic solids, as shown by Rivlin and Thomas<sup>8</sup>. Moreover, while most authors acknowledge the presence of long fibrils in the debonding region, these are not explicitly included in the modeling. This observation however clearly suggests an important role for the large strain mechanics and non-linear rheology of the adhesive in the work of debonding, as suggested by Gent and Petrich<sup>2</sup>.

The aim of this work is to reexamine the physics of these different modelings in light of the recent developments in the mechanics of soft materials and large strain rheology.

## 1. Angular dependency

In order to understand the coupling between geometry, loading and viscoelastic dissipation, we perform peeling experiments on a well-known commercial PSA (3M 600, used in most of our previous investigations<sup>9-11</sup>) in which the effects of the peeling angle  $\theta$  and the peeling velocity  $V$  on the peeling force  $F$  are examined (cf. figure 1). The strain energy release rate is calculated through:

$$G = \frac{F}{b}(1 - \cos \theta)$$

which provides the adherence energy  $\Gamma$  in steady-state fracture propagation.

The collapse of the steady-state propagation data on a master curve indicates separability between angular and peeling velocity dependencies. The angular dependency is found to be consistent with the prediction of Kaelble's model<sup>1</sup>, which attributes this effect to the variations of the bond stress distribution, combined with a propagation criterion based on a critical stress at the peeling front.

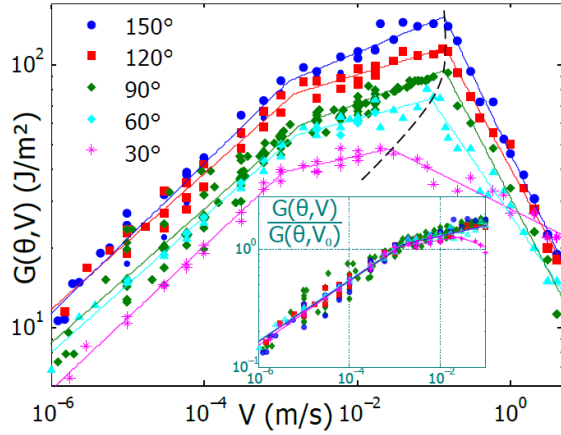


Figure 1. Energy release rate  $G$  for 3M 600 Scotch tapes as a function of the peeling velocity  $V$  and angle  $\theta$ . Power-law fits (straight lines) are used as guides for the eye. The negative slope branches are systematically associated with stick-slip. Insert: energy release rates normalized by their values at  $V_0 = 1$  mm/s.

## 2. Large strain rheology

In order to identify the impact of large strain rheology effects on the adherence energy, we perform peeling experiments at fixed loading geometry ( $\theta = 90^\circ$ ) on a series of custom made PSA in which linear and non-linear rheology are modified as independently as possible, yet remaining close to the rheology of a commercial PSA (cf. table 1 and figure 2).

Name	EHA	MA	AA	CL	Tg
1A	70%	25%	5%	0.2%	-34±4°C
1B	70%	25%	5%	0.4%	-34±4°C
2A	85%	10%	5%	0.2%	-43±5°C
2B	85%	10%	5%	0.4%	-43±5°C
3A	95%	0%	5%	0.2%	-54±8°C
3B	95%	0%	5%	0.4%	-54±8°C

Table 1. Formulation of the six custom-made adhesives. EHA stands for 2-ethyl hexyl acrylate, MA for methyl acrylate, AA for acrylic acid, CL for cross-linker. The glass transition temperatures ( $T_g$ ) are measured by DMA.

When normalizing the data by the values at the onset of stick-slip,  $V_c$  and  $G_c$ , all the curves collapse to two different master curves A and B, corresponding respectively to the higher and lower cross-linker content. This is in agreement with the general prediction from Gent and Petrich<sup>2</sup>, which attribute the value of the work of debonding  $\Gamma$  to the product of the adhesive thickness  $a$  and the area below the stress-strain curve of the adhesive (i.e. the work of extension per unit volume  $W$ ):

$$\Gamma = aW = a \int_0^{\varepsilon_c} \sigma(\varepsilon, \dot{\varepsilon}) d\varepsilon$$

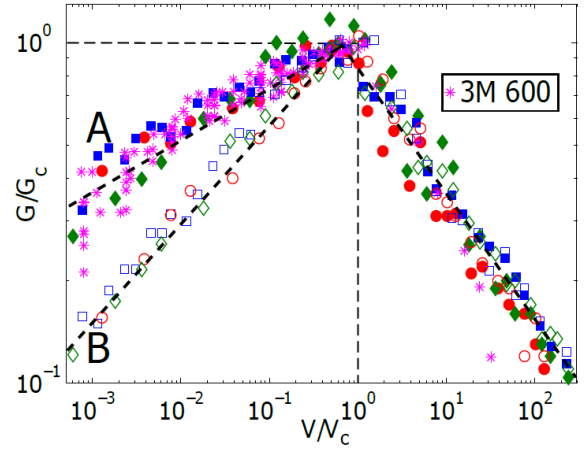


Figure 2. Energy release rate  $G$  of custom-made adhesives with different linear rheologies (different glass transition temperature  $T_g$ ) and different large-strain rheologies (different density of cross-linkers), cf. table 1. Full symbols correspond to 0.2% cross-linking (A tapes) and empty symbols correspond to 0.4% cross-linking (B tapes). Green diamonds correspond to tapes 1A and 1B, blue squares to tapes 2A and 2B and red circles to tapes 3A and 3B. The data of 3M 600 from fig. 1 are (at  $\theta = 90^\circ$ ) also added.

The observed systematic decrease of the work of debonding  $\Gamma$  when increasing the density of cross-linker can thus be explained by the reduction of the maximum extensibility  $\varepsilon_c$  of the fibrils, which results in a reduction of the work of extension as sketched in figure 4a. We remark that this effect is observed even on adhesives possessing the same linear rheology (same  $T_g$ ) and is thus a clear manifestation of the influence of the large strain rheology on the adhesive performances.

## 3. Imaging the fibrillated zone

During all these peeling experiments, we perform microscopic visualizations of the bond joint in order to monitor the size and shape of the fibrillated zone (cf. figure 3).

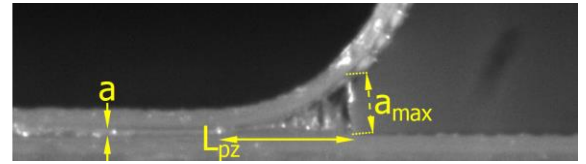


Figure 3. Microscopic visualization of the bond joint.

The aspect ratio of the fibrillated zone is very stable. The size of the fibrillated zone is almost independent on the peeling angle, but it decreases with the peeling velocity and when increasing the cross-linker content. These features are in agreement with the interpretation provided in the previous section. The size of the fibrillated zone is dominated by the maximum extension of the fibrils, which is both decreased when increasing the cross-linker content (fig. 4a) or the peeling velocity, which has the effect of increasing the stretch ratio  $\dot{\varepsilon}$  of the adhesive (fig. 4b). We remark that the

increase of the peeling velocity reduces the effect of the cross-linker density in a coherent way.

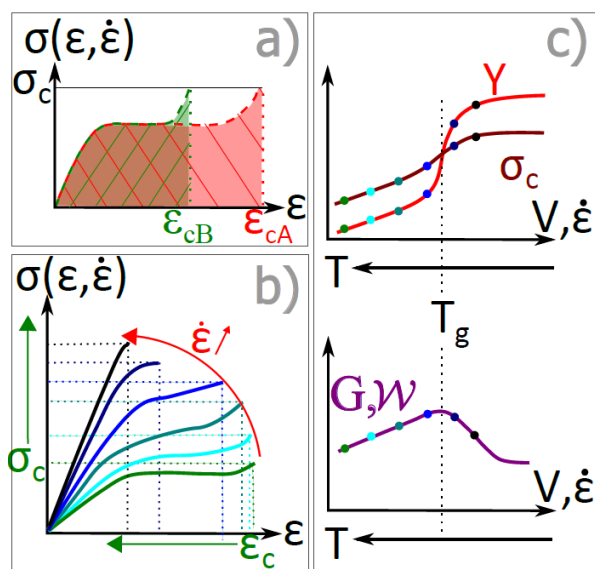


Figure 4. Schematic representation of the effect of the large strain rheology on the work of debonding.

#### 4. Modeling and discussion

By soft mechanics arguments, we can justify that the first modeling approach detailed above<sup>1-3</sup> is the most relevant for describing the steady-state peeling mechanics of soft confined adhesives. The fact that the elasto-adhesive length  $\Gamma/Y$  of the adhesive (where  $Y$  is the velocity dependent Young storage modulus) is smaller than the thickness  $a$  of the adhesive layer, prevents the development of the LEFM stress singularity<sup>12</sup>. The strong geometrical confinement has several effects. On the one hand, it induces a lateral correlation of the stress fields that makes the (visco)elastic foundation an adequate modeling of the response of the adhesive layer. On the other hand, it induces an oedometric stiffening of the adhesive, which can only be released by the observed cavitation and fibrillation of the adhesive.

The use of the (visco)elastic foundation combined with a fibril debonding criterion (such as a maximum stress) allows a sound interpretation of the dissipation during the peeling of a soft viscoelastic adhesive, which can essentially be attributed to a (visco)elastic hysteresis mechanism, *i.e.* to the fact that the work of extension of each fibril is essentially lost at the moment of its debonding. The measured work of peeling  $\Gamma$  is thus related to the whole process of deformation and debonding of the adhesive rather than to a simple viscoelastic amplification of the interfacial adhesion energy (as in the second class of models). This justifies the dependency on the adhesive thickness, on the peeling angle and on the large strain rheology of the adhesive. The peak in the  $\Gamma(V)$  curve is attributed to a peak in the work of extension  $W(\dot{\epsilon})$  as sketched in fig. 4c<sup>13</sup>.

Each of the discussed models provide some key ingredients that should guide the development of a thorough modeling able to capture all the elements of the subtle mechanisms of debonding of PSA, based on soft and confined viscoelastic solids. However, none of them can be fully satisfactory since they are mostly related to the bulk rheology of the adhesive. Although the cavitation and fibrillation mechanisms were frequently acknowledged, their deep effect on the adhesive response has only been investigated using the probe tack test geometry<sup>14</sup>. The combination of well controlled peeling tests with probe tack tests is thus a very promising perspective towards a sound quantitative mechanical modeling of the peeling energy.

#### Acknowledgements

This work was supported by the French ANR Grant "STICKSLIP" no. 12-BS09-014. We thank L. Vanel and S. Santucci for interesting discussions.

#### References

1. D.H. Kaelble, *J. Coll. Sci.*, 1964, **19**, pp 413-424.
2. A.N. Gent and R.P. Petrich, *Proc. Roy. Soc. A: Math. Phys. Eng. Sci.*, 1969, **310**, pp 433-448.
3. C. Derail, A. Allal, G. Marin and P.H. Tordjeman, *J. Adhes.*, 1998, **68**, pp 203-228.
4. R. Schapery, *Int. J. Fract.*, 1975, **11**, pp 141-159.
5. P.G. de Gennes, *CR Acad. Sci. SII*, 1988, **307**, pp 1949-1953.
6. B. Persson and E. Brener, *Phys. Rev. E*, 2005, **71**, Art. n. 036123.
7. D.H. Kaelble, *J. Adhes.*, 1992, **37**, pp 205-214.
8. R.S. Rivlin and A.G. Thomas, *J. Polym. Sci.*, 1953, **10**, pp 291-318.
9. M. Barquins and M. Ciccotti, *Int. J. Adhes. Adhes.*, 1997, **17**, pp 65-68.
10. P.P. Cortet, M. Ciccotti and L. Vanel, *J. Stat. Mech.: Th. Exp.*, 2007, Art. n. P03005, pp. 1-19.
11. P.P. Cortet, M.J. Dalbe, C. Guerra, C. Cohen, M. Ciccotti, S. Santucci and L. Vanel, *Phys. Rev. E*, 2013, **87**, Art. n. 022601.
12. C.Y. Hui, A. Jagota, S.J. Bennison and J.D. Londono, *Proc. Roy. Soc. London SA: Math. Phys. Sci.*, 2003, **403**, pp 1489-1516.
13. R. Villey, C. Creton, P.P. Cortet, M.J. Dalbe, T. Jet, B. Saintyves, S. Santucci, L. Vanel, D.J. Yarusso and M. Ciccotti, *Soft Matter*, 2015, **11**, 3480-91.
14. H. Lakrout, P. Sergot and C. Creton. *J. Adhes.*, 1999, **69**, pp 307-359.